

## Magnetoresistance and structural study of electrodeposited Ni-Cu/Cu multilayers

M. Jafari Fesharaki<sup>a,b,c</sup>, L. Péter<sup>a</sup>, T. Schucknecht<sup>d</sup>, D. Rafaja<sup>d</sup>, J. Dégi<sup>a</sup>, L. Pogány<sup>a</sup>,  
K. Neuróhr<sup>a</sup>, É. Széles<sup>e</sup>, G. Nabiyouni<sup>b</sup>, I. Bakonyi<sup>a,\*</sup>

*a. Research Institute for Solid State Physics and Optics, Hungarian Academy of Sciences.*

*H-1525 Budapest P.O. Box 49, Hungary*

*b. Department of Physics, Faculty of Science, Arak University. Arak 38156-8-8349, Iran*

*c. Department of Physics, Faculty of Science, Payame Noor University.*

*Zarinshahr 74718-191, Iran*

*d. Institute of Materials Science, TU Bergakademie Freiberg.*

*Gustav-Zeuner-Str. 5, D-09599 Freiberg, Germany*

*e. Institute of Isotopes, Hungarian Academy of Sciences.*

*H-1525 Budapest, P.O. Box 77, Hungary*

**Abstract** - Electrodeposition was used to produce Ni-Cu/Cu multilayers by two-pulse plating (galvanostatic/potentiostatic control) from a single sulfate/sulfamate electrolyte at an optimized Cu deposition potential for the first time. Magnetoresistance measurements were carried out at room temperature for the Ni-Cu/Cu multilayers as a function of the Ni-Cu and Cu layer thicknesses and the electrolyte Cu<sup>2+</sup> ion concentration. Multilayers with Cu layer thicknesses above 2 nm exhibited a giant magnetoresistance (GMR) effect with a dominating ferromagnetic contribution and with low saturation fields (below 1 kOe). A significant contribution from superparamagnetic (SPM) regions with high saturation fields occurred only for very small nominal magnetic layer thicknesses (around 1 nm). The presence of SPM regions was concluded from the GMR data also for thick magnetic layers with high Cu contents. This hints at a significant phase-separation in Ni-Cu alloys at low-temperature processing, in agreement with previous theoretical modeling and experiments. Low-temperature measurements performed on a selected multilayer down to 18 K indicated a strong increase of the GMR as compared to the room-temperature GMR. Structural studies of some multilayer deposits exhibiting GMR were performed by X-ray diffraction (XRD) and transmission electron microscopy (TEM). The XRD patterns of Ni-Cu/Cu multilayers exhibited in most cases clear satellite peaks, indicating a superlattice structure which was confirmed also by cross-sectional TEM. The deterioration of the multilayer structure revealed by XRD for high Cu-contents in the magnetic layer confirmed the phase-separation concluded from the GMR data.

**Keywords:** Electrodeposition; Ni/Cu multilayers; Giant magnetoresistance (GMR); Structural characterization

---

\* Corresponding author. E-mail: bakonyi@szfki.hu

## Introduction

Structures composed of alternating layers of ferromagnetic (FM) and non-magnetic metals have been intensively studied in recent decades. The main reason for this interest is based on the giant magnetoresistance (GMR) effect associated with such metallic multilayers.<sup>1</sup> In most cases, the metallic multilayers have been produced by using physical deposition techniques (sputtering, MBE, evaporation).<sup>2,3</sup> Although these techniques allow high-quality structures to be obtained, they are complex and expensive. Electrodeposition has long been shown to be a valuable technique for obtaining metallic multilayers<sup>4</sup> since it offers a simple, flexible and cheap process for their fabrication. Electrodeposited (ED) magnetic/non-magnetic multilayers with GMR can be conveniently obtained with the help of two-pulse plating from a single bath where the deposition potential or current density is varied rapidly.<sup>4-6</sup> Various two-pulse combinations (G/G, P/P and G/P)<sup>6,7</sup> have been applied for producing ED multilayers with GMR where G and P denotes galvanostatic and potentiostatic control, respectively, and the combination A/B refers to the sequence magnetic layer/non-magnetic layer. Whereas the ED process can be controlled to produce a pure non-magnetic layer by the single-bath technique, the magnetic layer in ED multilayers contains typically a few atomic percent of the non-magnetic element.

It has been pointed out in earlier works<sup>6-8</sup> that a proper control of the individual layer thicknesses and layer compositions during the electrodeposition of magnetic/non-magnetic multilayers requires the deposition of the more noble (non-magnetic) layer (usually Cu) under potentiostatic (P) control and an optimization of the potential applied for the non-magnetic layer deposition. This optimization implies the finding of a Cu deposition potential where neither a dissolution of the previously deposited magnetic layer nor an incorporation of the magnetic elements into the non-magnetic layer occurs.<sup>8</sup> This optimization is especially crucial for ED Co-Cu/Cu multilayers<sup>6</sup> due to the nearly reversible deposition and dissolution of Co, which defines an approximately 30 mV potential interval for Cu deposition in which Co remains intact.

As far as ED Ni-Cu/Cu multilayers are concerned, numerous studies have been reported on their GMR behavior<sup>9-31</sup> but in none of the studies the optimum Cu deposition potential has been established yet.<sup>6</sup> Although the Ni dissolution rate is much smaller than that of Co, a non-optimized potential can also lead to the incorporation of Ni into the non-magnetic layer which is definitely deleterious for GMR. Furthermore, if the deposition of the Cu layers is carried

out in G mode, the so-called exchange reaction<sup>6,8,25,32</sup> can lead to drastic changes of both layer thicknesses with respect to the nominal values even in ED Ni-Cu/Cu multilayers.<sup>25</sup>

A detailed discussion of the GMR of previous studies on ED Ni-Cu/Cu multilayers has been given in Section 5.7 of our recent review<sup>6</sup> and, therefore, some aspects of earlier results will only be summarized here. In many of these earlier works,<sup>11,12,15,18,19,23</sup> a G/G pulse combination was used to obtain these multilayers from a sulfate/citrate bath and in such cases, due to the galvanostatic control for Cu deposition, an exchange reaction definitely took place. This leads to an alteration of the individual layer thicknesses with respect to the nominal values and whereas GMR values of comparable magnitude as in other studies could be obtained, one cannot rely on the observed layer thickness dependence of GMR from these works. The other majority of GMR results was obtained on ED Ni-Cu/Cu multilayers prepared from sulfate/sulfamate electrolytes in P/P mode.<sup>9,10,14,16,17,20-22,24</sup> It appears from Table 5 of Ref. 6 that the applied Cu deposition potentials of these previous studies were either more positive (enabling a significant dissolution of Ni from the previously deposited magnetic layer) or more negative (promoting the codeposition of Ni into the non-magnetic layer) than the optimum potential range established in the present study for a sulfate/sulfamate bath (see the Experimental section) to exclude the above mentioned reactions during the Cu deposition cycle. The situation described above instigated us to carry out a systematic study of GMR in ED Ni-Cu/Cu multilayers prepared at the optimum Cu deposition potential so that the true evolution of GMR with individual layer thicknesses can be established.

In this work, the results of magnetoresistance (MR) studies of Ni-Cu/Cu multilayers grown by electrodeposition from a sulfate/sulfamate bath in G/P mode will be presented. A systematic study of the MR characteristics is described for ED Ni-Cu/Cu multilayers as a function of the magnetic (Ni-Cu) and the non-magnetic (Cu) layer thicknesses. Furthermore, the influence of  $\text{Cu}^{2+}$  ion concentration of the electrolyte on the GMR characteristics of ED Ni-Cu-Cu multilayers was also studied and, for a selected multilayer, the MR measurements were extended to low temperatures as well. X-ray diffraction (XRD) and transmission electron microscopy (TEM) measurements were used to investigate the layered structure of some of the deposits.

## Experimental

*Electrochemical bath.* — Most of the Ni-Cu/Cu multilayers investigated here were deposited from an electrolyte having a constant concentration of the constituents: NiSO<sub>4</sub> (0.8 mol/l), CuSO<sub>4</sub> (0.015 mol/l), H<sub>2</sub>NSO<sub>2</sub>OH (1.0 mol/l) and H<sub>3</sub>BO<sub>3</sub> (0.4 mol/l). The only exception was a multilayer series in which the CuSO<sub>4</sub> concentration was varied from 0.015 mol/l to 0.1 mol/l. The electrolyte used is similar to the sulfamic acid baths commonly found in the literature.<sup>6</sup> However, instead of the expensive nickel sulfamate, the bath was mixed from the fairly inexpensive nickel sulfate and the cheap sulfamic acid.

The NiSO<sub>4</sub>·7H<sub>2</sub>O chemical used was of analytical grade from Reanal, Hungary and its composition was analyzed by using a double focusing magnetic sector inductively coupled plasma mass spectrometer (ICP-SFMS) equipped with a single electron multiplier (ELEMENT2, Thermo Electron Corp., Germany). All measurements were carried out in medium resolution mode ( $m/\Delta m = 4000$ ) for decreasing the polyatomic interferences. For sample introduction, a Conical nebulizer (with a flow rate of approximately 1 ml min<sup>-1</sup>) in combination with a Scott-type spray chamber was applied. Multielemental standard stock solution (Merck, Germany) was used for calibration and rhodium (Rh) in 1 ppb concentration was applied as an internal standard in both the samples and the standards during the measurements.

The major impurity in the NiSO<sub>4</sub>·7H<sub>2</sub>O chemical was Co (2110 wt. ppm with respect to Ni), all other elements analyzed remained below the 1000 ppm level (Na: 702 ppm; Ca: 115 ppm; Mg: 113 ppm; Sb: 59 ppm; Mn: 4.5 ppm; Fe: 5 ppm; the rest of the elements analyzed were of the 1 ppm level or even much less). Due to the presence of about 0.2 at.% Co with respect to Ni in the starting Ni sulfate, we can expect some Co contamination in the deposits similarly as found previously in ED Ni-Cu/Cu multilayers<sup>18</sup> prepared by using NiSO<sub>4</sub> from the same supplier (Reanal). However, for simplicity, the magnetic layer will be termed as a Ni-Cu alloy only.

The solution for electrodeposition was prepared with deionized water ( $\rho \geq 18 \text{ M}\Omega\text{cm}$ ). The electrolyte was not stirred during deposition and its temperature was kept constant at  $22 \pm 1 \text{ }^\circ\text{C}$ . The electrolyte pH was adjusted to 2.5 by adding NaOH to the solution. The choice of this pH value is based on some literature reports<sup>6</sup> according to which the proper pH value is somewhere between 2 and 4.

*Electrodeposition conditions.* — All electrochemical experiments and the deposition processes were carried out at room temperature in a three-electrode electrochemical cell

equipped with a Cu foil as a counter electrode and a saturated calomel electrode (SCE) as reference. For preliminary electrochemical experiments, the working electrode was a 30  $\mu\text{m}$  thick polycrystalline Cu sheet whereas for multilayer deposition a (100)-oriented silicon wafer with a thickness of 260  $\mu\text{m}$  was used whereby the latter was coated with a Cr adhesive and a Cu seed layer by evaporation technique [Si/Cr(5nm)/Cu(20nm)]. The polarization investigations were performed by using an EF453 potentiostat/galvanostat (Electroflex, Hungary) which also served as a power source for both direct-current (d.c.) deposition and pulse-plating experiments. The deposition was performed in a columnar cell of 7 mm by 20 mm cross section with an upward looking cathode at the bottom of the cell.<sup>7,33</sup> The number of bilayers in the multilayers was varied in a manner as to give a total multilayer thickness of about 0.8  $\mu\text{m}$  in each case.

The multilayers were produced by a G/P pulse combination.<sup>6,7</sup> The magnetic Ni-Cu layer was deposited with a current density ( $j_{\text{Ni-Cu}}$ ) of -50 mA/cm<sup>2</sup>. The application of a constant current pulse can be justified by the following arguments: (i) The ohmic drop between the working and reference electrodes is of no importance here; (ii) There is no need for real-time current integration within the fairly short high-current pulse in order to keep the layer thickness constant; (iii) The constant current provides an even layer composition in the growth direction.

It was established from some preliminary electrochemical experiments that the codeposition of Ni with Cu cannot take place if  $E_{\text{Cu}}$  is more positive than -0.62 V whereas the dissolution of Ni and Co-Ni alloys with less than 10 at.% Co content starts only if  $E_{\text{Cu}}$  becomes more positive than -0.4 V. The current transients recorded for the P pulse in the above potential range showed an approximately 200 mV wide suitable potential interval for the Cu layer deposition. The potential chosen ( $E_{\text{Cu}} = -0.5$  V) was selected to lie in the middle of this interval. This ensured that the individual layer thicknesses could be reliably determined from the electrodeposition conditions whereby a current efficiency of 95 % (Ni-Cu layer) and 100 % (Cu layer) was assumed.

*Sample series produced and their compositional analysis.* — Three series of samples were produced for the present studies. Series B and H consisted of multilayers produced by using the constant bath composition given above. In series B, the magnetic layer thickness ( $d_{\text{Ni-Cu}}$ ) was fixed at 3.0 nm and the non-magnetic layer thickness ( $d_{\text{Cu}}$ ) was varied from 1.2 nm to 6.5 nm. In series H, the non-magnetic layer thickness was fixed at 4.2 nm and the magnetic layer thickness was varied from 1.0 nm to 5 nm.

Multilayers in series G were intended for investigation of the influence of magnetic layer composition (primarily, the Ni:Cu ratio) on the magnetoresistance. For this purpose, multilayers were produced from baths with different  $\text{Cu}^{2+}$  concentrations obtained by gradually adding  $\text{CuSO}_4$  to a fixed volume (100 ml) of the electrolyte. The starting  $\text{Cu}^{2+}$  concentration was 0.015 mol/l as used for the preparation of the previously described multilayers (series B and H). Several baths with  $\text{Cu}^{2+}$  concentrations up to 0.1 mol/l were prepared by  $\text{CuSO}_4$  additions from which ED Ni-Cu(3nm)/Cu(4.2nm) multilayers (series G) were grown under the same conditions as the multilayers in series B and H.

As reference material, a bulk Ni-Cu alloy deposit with the same thickness as the typical multilayer thickness (about 800 nm) was also prepared by d.c.-plating from the bath used for multilayer series B and H and by using the same current density as for the magnetic layers of the multilayers. Due to the identical deposition conditions, the composition of the d.c.-plated Ni-Cu alloy was expected to be approximately the same as that of the magnetic layer in multilayers of series B and H (although it is obvious that the steady-state deposition conditions are never achieved during the pulsed deposition of the multilayers).

The elemental analysis of the deposits was performed by using a RÖNTEC electron probe microanalysis (EPMA) facility in a JSM840 scanning electron microscope. The composition of several regions of the deposits was determined and an average of these values was taken. The chemical analysis of the deposits of the present study has confirmed the presence of some Co contamination of the deposits. The composition of the magnetic layer was calculated by taking into account the nominal thickness of each layer and by assuming the formation of pure Cu layers. This calculation led to the result that the magnetic layer for series B and H contained about 7 at.% Cu and 9 at.% Co.

*Magnetoresistance measurements and structural studies.* — Room-temperature MR measurements were performed by applying a magnetic field up to  $H = \pm 8$  kOe in the current-in-plane/field-in-plane (CIP/FIP) configuration. D.c. current was applied in a four-point-in-line probe in the multilayer film plane. The MR ratio was defined as  $\Delta R/R_0 = (R_H - R_0)/R_0$  where  $R_0$  is the film resistance in the absence of a magnetic field and  $R_H$  is the film resistance at a magnetic field  $H$ . Both the longitudinal (L) and transverse (T) components of the MR (LMR and TMR, respectively) were measured by using a magnetic field parallel and perpendicular to the current flow direction, respectively. MR measurements at low temperatures down to 18 K were performed in a closed-cycle He cryostat.

On selected multilayers, structural studies were performed by using similar XRD and

TEM techniques as described recently for ED Co-Cu/Cu multilayers.<sup>34,35</sup> The main aim of the XRD measurements was to verify the layer thicknesses determined from the current density during the ED process and to judge the quality of the multilayers in terms of their periodicity, thickness fluctuations and continuity of individual layers. For that reason, the XRD patterns measured in the vicinity of the 111 and 200 peaks were fitted by using the approach described in Ref. 36. The most important features in the XRD patterns were (i) the distances between the satellite reflections giving information about the bilayer thickness and (ii) the intensities of the superlattice satellites giving information about the thickness fluctuations and continuity of individual layers.<sup>36-39</sup> The XRD measurements were carried out in symmetrical mode on a conventional Bragg-Brentano diffractometer (URD6 from Seifert/Freiburger Praezisionsmechanik) at the wavelength of 0.15418 nm (CuK $_{\alpha}$  radiation). The fluorescence radiation of the samples was reduced by a curved secondary graphite monochromator that was located in front of the scintillation detector. TEM was used mainly to visualize the morphology of the Ni-Cu/Cu interfaces. The TEM investigation was carried out on a JEM 2200 FS from JEOL at an acceleration voltage of 200 kV. TEM micrographs were taken on the cross sections of the samples, which were prepared in the face-to-face orientation by dimpling, ion milling and plasma cleaning.

### **Ni-Cu/Cu multilayers with varying Cu layer thickness (series B)**

*Room-temperature magnetoresistance results.* — Figure 1a shows the MR(H) curves for two multilayers from series B ( $d_{\text{Ni-Cu}} = 3.0$  nm): one with thin Cu layer ( $d_{\text{Cu}} = 1.2$  nm) and another one with thick Cu layer ( $d_{\text{Cu}} = 4.2$  nm). For  $d_{\text{Cu}} = 1.2$  nm, we can see that LMR  $> 0$  and TMR  $< 0$ , i.e., the magnetoresistance is dominated by the anisotropic magnetoresistance (AMR) effect.<sup>40-42</sup> The magnitude of the AMR is obtained as the difference between the saturation values LMR $_s$  and TMR $_s$  (these saturation parameter values are determined by extrapolating the linear high-field section of the measured MR(H) curves to  $H = 0$  as shown for  $d_{\text{Cu}} = 4.2$  nm by the dashed line in Fig. 1a). On the other hand, for  $d_{\text{Cu}} = 4.2$  nm, the magnetoresistance shows a clear GMR effect since in the whole range of magnetic fields, we have LMR  $< 0$  and TMR  $< 0$  (Ref. 6).

The occurrence of an AMR effect for the multilayer with thin Cu layers can be explained by assuming that at this Cu layer thickness there are discontinuities (pinholes) in the spacer layer through which a direct FM coupling of the adjacent magnetic layers occurs.<sup>43</sup> If this FM

coupling is active over sufficiently large lateral areas, the magnetic layers can be so effectively coupled that they behave as a bulk ferromagnet as it was observed also for ED Co/Cu multilayers at similarly thin Cu spacer layers.<sup>44</sup>

An AMR effect was observed also for the d.c.-plated Ni-Cu reference alloy deposited at the same current density as the magnetic layer in the multilayer. The AMR for the d.c. plated Ni-Cu alloy was close to the room-temperature value of pure Ni which is about 2 % (Ref. 42). When comparing the magnitude of the d.c.-plated alloy and that of pure Ni, we should take into account that, as mentioned in the experimental section, this alloy deposit actually contained a few at.% of both Co and Cu. Since Co alloyed to Ni is known to increase the AMR<sup>42</sup> whereas the addition of Cu to Ni reduces the AMR as calculated both theoretically<sup>45</sup> and shown also experimentally,<sup>18</sup> the final value is determined by the competition of the two counteracting effects.

It can be inferred from Fig. 1a that the magnitude of the AMR effect in the multilayer with  $d_{\text{Cu}} = 1.2$  nm is much smaller (about 1 %) than that of the d.c. plated alloy (about 2 %). It is believed that one source of the observed discrepancy is that there may be also relatively large pinhole-free regions in the spacer layer where the FM coupling is not able to completely align adjacent layer magnetizations and these regions can give rise to a GMR contribution. This is supported by our common experience on various multilayers that the longitudinal MR component always changes (reduces) to much larger extent than does the transverse component. Since for an AMR contribution we have  $\text{LMR} > 0$  and  $\text{TMR} < 0$  whereas for a GMR contribution we have  $\text{LMR} < 0$  and  $\text{TMR} < 0$ , this can only happen if the observed MR is the result of the simultaneous presence of both an AMR and a GMR contribution. However, we cannot exclude another possible source of the difference between AMR values. This additional contribution may have its origin in the fact that when adding Cu layers (of whatever small thickness) to bulk Ni (or the Ni(Co) alloy), we introduce interfaces in the sample (whether continuous layers at large Cu thicknesses or Cu islands for small Cu thicknesses) which represent an additional source of electron scattering and give rise to an increase of the resistivity.<sup>44,46</sup> Therefore, when calculating the MR ratio, we should divide then by a larger zero-field resistance value which should naturally lead to a smaller MR ratio. It is, however, hard to estimate to what extent one or the other mechanism is responsible for the observed difference of the AMR values but we can ascertain that, most probably, both mechanism contributes to it.

For all multilayers exhibiting GMR (for  $d_{\text{Cu}}$  above about 2 nm), the MR(H) curves had

the same character as for the sample with  $d_{\text{Cu}} = 4.2$  nm shown in Fig. 1a: above saturation, which is reached at about 1 to 2 kOe, the MR(H) curves are approximately linear. This indicates that the dominant contribution to the GMR comes from spin-dependent scattering events of electron transitions between adjacent FM layers.<sup>47</sup>

It should be pointed out that the MR(H) curves of the currently investigated multilayers (see, e.g., Fig. 1a) are especially narrow for Cu layer thicknesses with the largest GMR ( $d_{\text{Cu}} = 3.5$  and 4.2 nm). In line with this, the saturation fields are much smaller than in any of the previously studied ED Ni-Cu/Cu multilayers for which MR(H) curves were reported at all.<sup>9,14,15,18-23,25,27,29-31</sup> This implies a superior quality of the present multilayers with respect to previous studies.

The saturation values of the multilayer LMR and TMR components are displayed in Fig. 1b for the Ni-Cu/Cu multilayer series B with constant magnetic layer thickness as a function of the Cu layer thickness. These data show qualitatively the same behavior as reported for ED Co-Cu/Cu multilayers<sup>44</sup>: an AMR behavior is obtained for thin Cu layers which enable a direct FM coupling between the magnetic layers whereas GMR occurs for thick Cu layers (here above about 1.5 nm thickness) and no sign of an oscillatory GMR behavior can be revealed. Similarly to the ED Co-Cu/Cu multilayers, the explanation should be the same also here in that thick non-magnetic layers provide a sufficient separation of the magnetic layers to prevent a FM coupling between them. The lack of GMR maxima and minima hints at the absence of an alternation of antiferromagnetic (AF) and FM exchange coupling with varying spacer thickness. In such an uncoupled case, the random orientation of adjacent layer magnetizations provides sufficient antiparallel alignment in zero field to observe a GMR effect.<sup>44</sup> The position of the GMR maximum for ED Ni-Cu/Cu multilayers (Fig. 1b) appears for about the same Cu layer thicknesses as observed for ED Co-Cu/Cu multilayers.<sup>44</sup>

The magnitude of the maximum GMR in our ED Ni-Cu/Cu multilayers compares well with the results of most previous studies<sup>9,11,12,15,18-24</sup> where typically GMR values ranging from 1 to 3 % were reported for this preparation technique.

As to the Cu layer thickness dependence of GMR in ED Ni-Cu/Cu multilayers, relatively few previous reports contain data in this respect. It was found in our previous reports<sup>12,15,19</sup> that, similarly to the present results (see Fig. 1b), the GMR exhibits a single maximum as a function of the spacer thickness but the position of the maximum is at lower Cu layer thicknesses (1.5 to 3 nm) as here. Since in these previous works G/G method was used, as a consequence of the unavoidable exchange reaction, the actual layer thicknesses are larger than

the nominal one, this complies well with the present data. On the other hand, there are two reports with an oscillatory behavior of GMR in ED Ni-Cu/Cu multilayers. Bird and Schlesinger<sup>10</sup> reported an oscillatory behavior for both ED Co-Cu/Cu and Ni-Cu/Cu multilayers but first, their GMR values could never be reproduced by any laboratories and, second, their brief report does not contain sufficient details (e.g., no MR(H) curves were presented) to properly assess the validity of their GMR values and the eventual contribution of SPM regions the presence of which can completely alter the spacer layer thickness dependence as we analyzed for ED Co-Cu/Cu multilayers.<sup>44</sup> Lashmore et al.<sup>9</sup> also observed an oscillatory behavior but with lower GMR magnitudes comparable to other studies. The first GMR maximum appeared at about 0.9 nm. However, the actual value of this spacer thickness is definitely higher since their Cu deposition potential was so positive that a significant exchange took place. Furthermore, for the same sample series, these authors have also reported the dependence of the full width at half maximum (FWHM) of the MR(H) curves on the Cu layer thickness. The width of the MR(H) curve can be considered as proportional to the saturation field of the magnetoresistance. However, the FWHM data of Lashmore et al.<sup>9</sup> indicated a minimum at spacer thicknesses corresponding to GMR maxima which is just the opposite to the case oscillatory GMR for physically deposited multilayers since for these latter the saturation field also has a maximum at the GMR maximum. Therefore, we have to conclude that although a  $GMR_{FM}$  term provides the dominant contribution to the observed GMR in the ED Ni-Cu/Cu multilayers studied by Lashmore et al.,<sup>9</sup> the reported oscillatory behavior cannot be considered as originating from an oscillatory exchange coupling. It should be noted that a large GMR value can originate also from a strong SPM contribution due to a fragmentation of the magnetic layer which can be especially pronounced if both types of layers are fairly thin as reported for ED Ni-Cu/Cu multilayers.<sup>22</sup>

The AMR magnitude is also indicated in Fig. 1b and it has a nearly constant value of about 0.5 % for all multilayers with GMR. This corresponds to expectation since the AMR arises due to spin-dependent scattering within the nominally identical magnetic layers in the whole range of sufficiently large spacer layer thicknesses (GMR regime).

*Structural results.* — The XRD studies carried out for two multilayers of series B give strong support for the considerations deduced above from the magnetoresistance data. The XRD patterns measured in the vicinity of the 111 and 200 peaks are shown in Fig. 2 for the Ni-Cu(3nm)/Cu(6.5nm) and Ni-Cu(3nm)/Cu(1.2nm) multilayers. The strongest peaks correspond to the Bragg maxima of the multilayer structure and their positions are determined

by the mean interplanar spacing averaged over the whole multilayer stack. Satellite peaks of various intensity and width can also be observed around the main peaks for both samples and their distances reflect the periodicity of the multilayers.<sup>38,39</sup>

According to Ref. 36, the XRD pattern of multilayer Ni-Cu(3nm)/Cu(1.2nm), for which a discontinuous spacer layer was assumed above, appears like having extremely high fluctuations of the spacer thickness. Namely, in the case of such fluctuations, the intensity of the satellite peaks should decrease steeply with the distance from the respective Bragg maximum as evidenced by the lower curves in Fig. 2. If these fluctuations are very strong, a discontinuity of the spacer layer can indeed happen as the occurrence of a dominating AMR effect here indicates.

Furthermore, the XRD patterns revealed that also multilayers with thicker Cu layers exhibit a fairly large variation of the spacer thickness. Although more superlattice satellites can be observed in the Ni-Cu(3nm)/Cu(6.5nm) multilayer than in the Ni-Cu(3nm)/Cu(1.2nm) multilayer (compare the upper and lower curves in Fig. 2), this fact can be mainly attributed to the larger bilayer thickness and smaller distance between the superlattice satellites in Ni-Cu (3 nm)/Cu (6.5 nm). Still, the intensity reduction aside the Bragg maxima is similar in both multilayers, which means that the fluctuations of the number of atomic planes per layer, i.e., the fluctuation of the individual layer thicknesses, are similar in both multilayers.<sup>37</sup> In multilayers with very thin spacer layers, large fluctuations of the spacer layer thickness (i.e., of the number of atoms in the spacer) lead to the spacer layer discontinuity. Obviously, the same degree of fluctuation of the spacer layer thickness in multilayers with thicker spacer layers does not lead to this effect.

In addition to the above discussed appearance of discontinuities in the spacer layer which lead to an AMR effect, the existence of significant layer thickness fluctuations can influence the magnetoresistance characteristics also for thick spacer layers (GMR regime). Namely, depending on the lateral length-scale of the layer thickness fluctuations, either a FM “orange-peel” coupling<sup>48</sup> may occur (for large-scale fluctuations or undulation) or, according to a model by Marrows and Hickey,<sup>49</sup> an orthogonal coupling between adjacent magnetic layers may develop if the appropriately small-scale layer thickness fluctuations result in an alternation of ferromagnetically and antiferromagnetically coupled regions. Both mechanisms result, of course, in a diminution of the GMR effect with respect to the possible maximum value (pure AF coupling resulting in an antiparallel alignment).

## Ni-Cu/Cu multilayers with varying Ni-Cu layer thickness (series H)

*Room-temperature magnetoresistance results.* — At the Cu layer thickness where the maximum GMR was obtained ( $d_{\text{Cu}} = 4.2$  nm, see Fig. 1b), Ni-Cu/Cu multilayers (series H) were prepared with varying magnetic layer thicknesses ( $d_{\text{Ni-Cu}}$ ) in order to see the evolution of GMR with  $d_{\text{Ni-Cu}}$ .

The MR(H) curves are shown in Fig. 3a for two multilayers from series H. For the largest magnetic layer thickness ( $d_{\text{Ni-Cu}} = 5$  nm), the bulk scattering within the thick magnetic layers (AMR effect) dominates the observed magnetoresistance (LMR > 0, TMR < 0). It should be noted, however, that the AMR magnitude for  $d_{\text{Ni-Cu}} = 5$  nm is only about half of the value obtained for the corresponding bulk Ni-Cu alloy. It was discussed for sample series B above that both the presence of a GMR term and an increased interfacial scattering contribution to the zero-field resistivity contribute to the reduced AMR in the multilayers with respect to the bulk value of the magnetic layer material. It is believed that the same explanation should prevail also for the case of series H.

For the other multilayers in series H ( $d_{\text{Ni-Cu}} = 1, 2, 3,$  and  $4$  nm), the MR(H) curves indicated a clear GMR effect since both the LMR and TMR values were negative in the whole range of magnetic field investigated. This is because the bulk contribution to the magnetoresistance due to electron scattering events entirely within the magnetic layer diminishes with decreasing Ni-Cu layer thickness and the GMR effect due to the nanoscale magnetic/non-magnetic multilayer structure becomes dominant as shown for  $d_{\text{Ni-Cu}} = 1$  nm in Fig. 3a. The evolution of the GMR for the multilayers of series H with magnetic layer thickness is shown in Fig. 3b which shows a continuous increase of the GMR with decreasing magnetic layer thickness. This is due to the fact that with reduced magnetic layer thickness the number of magnetic/non-magnetic transitions per unit thickness increases, i.e., there are larger chances for spin-dependent scattering events for electrons traveling between non-aligned neighboring magnetic layers through the non-magnetic spacer material.

For the multilayers with  $d_{\text{Ni-Cu}} = 2, 3$  and  $4$  nm, the shape of the MR(H) curves were very similar to the Ni-Cu(3nm)/Cu(4.2nm) multilayer of series B (see Fig. 1a) in that saturation was achieved in fairly low magnetic fields (around 1 kOe), beyond which field value a linear MR behavior was observed. However, the shape of the MR(H) curve for  $d_{\text{Ni-Cu}} = 1$  nm is already significantly different. For the MR(H) curve of multilayer Ni-Cu(1nm)/Cu(4.2nm) in Fig. 2a, there is no clear saturation field and no linear high-field

region which is certainly due to the small thickness of the magnetic layer. The shape of the MR(H) curve indicates that the observed GMR for the [Ni-Cu(1nm)/Cu(4.2nm)] multilayer contains also a contribution arising from the presence of superparamagnetic (SPM) regions in the magnetic layers.<sup>47</sup> By applying a decomposition procedure described in Ref. 47, the contributions from spin-dependent scattering events for electron paths through a non-magnetic spacer region between two FM regions ( $GMR_{FM}$  term) could be separated from those between a FM region and an SPM region ( $GMR_{SPM}$ ). For the longitudinal MR, the analysis yielded the following values:  $GMR_{FM} = 2.5 \%$ ,  $GMR_{SPM} = 1.0 \%$  and the average magnetic moment of the SPM regions was found to be 1870 Bohr magneton. The corresponding values for the TMR component were  $GMR_{FM} = 2.5 \%$ ,  $GMR_{SPM} = 1.2 \%$  and 1740 Bohr magneton. The fitted parameter values agree for the two components within the experimental error. These results show that for the multilayer Ni-Cu(1nm)/Cu(4.2nm) about 1/3 of the observed magnetoresistance arises due to the presence SPM regions. In Fig. 3b, the saturation MR values were taken for this multilayer as the sum of the  $GMR_{FM}$  and  $GMR_{SPM}$  contributions for each component.

The data demonstrate that, for such a low thickness, the Ni-Cu layer may become discontinuous or it may even consist mainly of nanoscale islands which are magnetically decoupled through the intermittently deposited Cu regions. From the absence of a significant AMR effect ( $LMR \sim TMR$  for the whole range of magnetic fields investigated) for the multilayer [Ni-Cu(1nm)/Cu(4.2nm)], we can conclude that the thin magnetic layer is probably discontinuous to the extent that there is hardly any chance for an electron to be scattered within the same magnetic region which would be a prerequisite to yield a contribution to the AMR.

The evolution of the AMR magnitude with magnetic layer thickness is also indicated in Fig. 3b. For multilayers with a predominantly FM contribution to the GMR, it has roughly the same magnitude (about 0.5 %) as for the GMR multilayers in series B (see Fig. 1b) but it becomes obviously much larger for the multilayer which has already a very thick magnetic layer ( $d_{Ni-Cu} = 5 \text{ nm}$ ). On the other hand, the AMR effect becomes very low for  $d_{Ni-Cu} = 1 \text{ nm}$  (Fig. 3b).

*Structural results.* — The above hypothesis about the discontinuous nature of the magnetic layer in the Ni-Cu(1nm)/Cu(4.2nm) multilayer is also supported by the results of the XRD analysis. In analogy with the Ni-Cu(3nm)/Cu(1.2nm) multilayer for which the superlattice satellites were very weak due to the laterally discontinuous (or interrupted) Cu

spacer layers (Fig. 2), the intensity of the superlattice satellites in the XRD pattern of the Ni-Cu(1nm)/Cu(4.2nm) multilayer (Fig. 4) is also reduced due to the laterally discontinuous Ni-Cu magnetic layers. In particular, the discontinuity of the magnetic layer is clearly exemplified by the disagreement of the measured and calculated intensities in the vicinity of the XRD line 200 for  $d_{\text{Ni-Cu}} = 1$  nm. Discontinuous magnetic or spacer layers were observed mainly in multilayers where either of the layers (magnetic or spacer) was very thin, or in multilayers with strongly unequal thicknesses of the magnetic and spacer layers. On the contrary, multilayers with similar thickness of the magnetic and spacer layers did not show such discontinuity.

The periodic nature of the main motif and the small degree of the fluctuation of the layer thicknesses in the Ni-Cu/Cu multilayers of series H (with similar  $d_{\text{Ni-Cu}}$  and  $d_{\text{Cu}}$ ) were also confirmed by a TEM study that was performed on the cross-section of the Ni-Cu(3nm)/Cu(4.2nm) multilayer (Fig. 5). As the diffraction contrast between Ni and Cu is very low (just one electron), the TEM image had to be recorded in strong underfocus, which leads to a change of the effective magnification of the microscope. Therefore, the layer thicknesses cannot be obtained from the defocused TEM micrograph.

### **Influence of magnetic layer composition on magnetoresistance and microstructure of Ni-Cu/Cu multilayers (series G)**

*Magnetoresistance evolution with magnetic layer composition.* — The composition of the magnetic layers (mainly the Ni:Cu ratio) in the ED Ni-Cu(3nm)/Cu(4.2nm) multilayers was varied by changing the concentration of the  $\text{Cu}^{2+}$  electrolyte as described in the Experimental section. A clear GMR effect was obtained for all bath compositions (and magnetic layer compositions) in that both the LMR and TMR components were negative (Fig. 6). However, the data in Fig 6 also demonstrate that there is a gradual decrease of the GMR with the increase of the  $\text{Cu}^{2+}$  concentration in the bath (Figs. 6a and 6b). The results of an overall chemical analysis of the multilayers (Fig. 7) revealed that an increasing  $\text{Cu}^{2+}$  concentration in the bath leads to an increase of the overall Cu content in the multilayers on the account of the magnetic elements. This excess Cu in the multilayer deposits is incorporated in the magnetic layers which, therefore, contain an increasingly higher amount of Cu whereas both the Ni and Co contents in the magnetic layers are reduced by about a factor of 2 (Fig. 7). This definitely should lead to a reduction of both the GMR and AMR

effects as, indeed, revealed by Fig. 6b. The high amount of Cu in the magnetic layers reduced substantially the XRD scattering contrast and the difference in the interplanar spacing between the magnetic and non-magnetic layers, thus no superlattice satellites were observed in the XRD pattern (Fig. 8) of a Ni-Cu(3nm)/Cu(4.2nm) multilayer deposited from a bath with 0.1 mol/l CuSO<sub>4</sub>.

According to Figs. 6a and 6b, even in the multilayer sample with the largest Cu content in the magnetic layer, a small but clear GMR effect can still be observed and, also, there is a small but finite AMR value. On the other hand, alloying Cu to Ni reduces approximately linearly the Curie point  $T_c$  which decreases to room temperature at about 30 at.% Cu<sup>46</sup> (due to the presence of some Co in the magnetic layer, however, the critical Cu content for suppressing ferromagnetism down to below room temperature may be somewhat higher). This means that for the multilayers with sufficiently high Cu-content in this series, the magnetic layer should be non-magnetic if the Ni, Co and Cu atoms are homogeneously distributed in the magnetic layer. Consequently, no magnetoresistance (neither AMR, nor GMR) is expected in the multilayers with the highest Cu contents at room temperature which is evidently not the case according to Figs. 6a and 6b. It should be, therefore, concluded from the observation of clear AMR and GMR effects that at high Cu contents in the electrolyte (and, consequently, in the Ni-Cu layer), the magnetic layer is not a homogeneous Ni-Cu alloy but rather consists of magnetic Ni-rich regions with Cu contents below about 30 at.% and non-magnetic Cu-rich regions with Cu-content higher than about 30 at.% (maybe even pure Cu regions).

For high Cu contents in the magnetic layer, however, not only the magnitude of the GMR decreased but also the broadening of the MR(H) peaks increased in the sense that the saturation field above which a linear behavior sets in increased from below 1 kOe to above 2 kOe. This indicates the appearance of a small SPM contribution to the GMR which, on the other hand, hints at the formation of SPM regions in the magnetic layer.<sup>47</sup> This implies again that the incorporation of the excess Cu in the magnetic layers is not homogeneous but rather there are strong compositional fluctuations within the magnetic layers. According to the previous paragraph, the magnetic layer becomes both chemically and magnetically heterogeneous with its increasing Cu content, and if the discontinuity reaches a level that nanometer-sized Ni-rich regions are separated from the rest of the magnetic layer, then actually SPM regions are formed.

The increasing amount of Cu in the magnetic layer also leads to a reduction of its

magnetization, or, in other words, to a decreasing amount of magnetic material in the multilayer. We can observe in line with this that the AMR also decreases with increasing Cu content in the magnetic layer (Fig. 6b). This is again in conformity with the fact that the multilayer GMR behavior gradually changes from FM to SPM character.

*Phase separation in the Ni-Cu system.* — The observed change in the GMR characteristics towards high Cu contents in the magnetic layer is very similar to that reported for ED Co-Cu/Cu multilayers.<sup>35,50</sup> Apparently, this phase separation tendency is governed by the degree of mutual solubility of the two components (magnetic and non-magnetic metal) codeposited. This was analyzed in detail previously<sup>35</sup> for the Co-Cu system for which the equilibrium phase diagram<sup>51</sup> shows almost negligible mutual solubility at room temperature.

According to the equilibrium phase diagram<sup>51</sup>, Ni and Cu are fully soluble (possess no miscibility gap) at high temperatures. However, phase diagrams obtained from thermodynamic modeling<sup>51,52,53</sup> by considering both the chemical (non-magnetic) and magnetic terms of the Gibbs energy indicate that below about 630 K there is a miscibility gap also in the Ni-Cu system. This maximum decomposition temperature was calculated for 67.3 at.% Ni whereas the calculated miscibility gap spans practically over the whole composition range at room temperature.

Chakrabarti et al.<sup>51,52</sup> note that “There is no direct experimental evidence to support the calculated miscibility gap. Attaining equilibrium condition at these low temperatures for these alloys is difficult, if not impossible”. Evidently, this statement refers to the fact that when cooling a high-temperature single-phase Ni-Cu alloy down to below the transition temperature, the phase separation kinetics is extremely small. This is the reason for the lack of firm evidence of the miscibility gap in bulk Ni-Cu alloys processed by metallurgical means.

Nevertheless, it has been known for some 40 years<sup>54-56</sup> on the basis of magnetic data via neutron scattering, magnetization and electrical transport measurements that bulk Ni-Cu alloys exhibit a tendency for the formation of Ni-rich segregations around the critical concentration of ferromagnetism (about 45 at.% Ni). This is usually explained in terms of the local environment model<sup>56</sup> according to which the total free energy of the system becomes lower, with respect to a homogeneous alloy, if the Ni atoms (or at least a fraction of them) segregate to form Ni-rich magnetic clusters and this provides a sufficient driving force for phase separation.

The situation seems to be quite different for the case of Ni-Cu alloys prepared by a low-temperature atom-by-atom deposition process where the slow kinetics of the diffusion is not a

limiting factor for the phase separation but rather the segregation tendency can manifest itself via the minimization of the total free energy of the system by creating Ni-rich magnetic clusters already during the formation of the solid. There have been several reports<sup>57-60</sup> on the observation of a miscibility gap in electrodeposited Ni-Cu alloy layers either in the as-deposited state or upon appropriate annealing treatment.

It should be noted, however, that an atom-by-atom deposition process does not necessarily always lead to a phase separation in the Ni-Cu system since this phenomenon depends on fine details of the electrodeposition process. Mizushima et al.<sup>61</sup> prepared electrodeposited Ni-Cu alloys with a homogeneous structure for all compositions and by using baths of widely different pH values. Kazeminezhad and Schwarzacher<sup>58</sup> revealed by magnetization measurements that the degree of Ni segregation as measured by the size of the magnetic moment per Ni atom in a nearly equiatomic electrodeposited Ni-Cu alloy varies substantially by the cathode potential applied during the alloy deposition.

All these results strongly support our conclusions that under the conditions applied during the preparation of our ED multilayers, the magnetic layers with high average Cu contents exhibit a substantial phase segregation. The degree of this phase decomposition depends apparently on alloy preparation details. Evidently, further studies are necessary to clarify the microscopic mechanism of this low-temperature phase separation. It should also be established whether the mostly unavoidable presence of Co impurity in ED alloys of Ni with Cu, as reported also in the present case, has significance for the observation of the phase separation in ED Ni-Cu alloys. This is a very important task since previous reports on this issue have not dealt with the problem of Co impurities whereas, in accordance with the equilibrium phase diagram of the Co-Cu system,<sup>51</sup> ED Co-Cu alloys have clearly demonstrated<sup>35,50</sup> a strong phase separation at room temperature.

### **Temperature dependence of GMR in Ni-Cu/Cu multilayers**

In order to investigate the effect of temperature on the GMR value, both longitudinal and transverse MR measurements were performed at temperatures between 301 and 18 K. Figure 9 shows the (a) LMR and (b) TMR curves for a multilayer Ni-Cu(3nm)/Cu(5nm). The MR(H) curves clearly show the monotonous increase in the GMR values as the temperature was reduced down to 18 K. The results on the temperature dependence of the LMR and TMR components are summarized in Fig. 10. A very similar behavior was described in our previous

report on ED Ni-Cu/Cu multilayers.<sup>23</sup>

Due to the definition of the magnetoresistance as  $\Delta R/R_0$ , a temperature dependence of the GMR can come about via the variation of both  $\Delta R$  which reflects the field dependence of the resistance through spin-dependent scattering effects and  $R_0$ , the zero-field resistance. The change of  $R_0$  for sputtered Ni/Cu multilayers with temperature was found to be about 20 to 30 % between 4.2 and 300 K.<sup>62</sup> Since in such Ni/Cu nanoscale multilayers the main contribution to the zero-field resistivity originates from interfacial scattering effects,<sup>46</sup> a reduction in temperature does not lead to a strong resistivity decrease as in bulk pure metals where the phonon contribution dominates the resistivity at high temperatures. According to a theory by Hasegawa,<sup>63</sup> the reduction of GMR with increasing temperature can be ascribed to enhanced spin fluctuations at higher temperatures. Kubota et al.<sup>62</sup> could verify this prediction experimentally for sputtered Ni-Co/Cu multilayers. The observed degree of temperature dependence of the GMR for our ED Ni-Cu/Cu multilayers (a change by a factor of about 2, see Fig. 10) approximately corresponds to that reported by Kubota et al.<sup>62</sup> for the sputtered Ni-rich Ni-Co/Cu multilayers.

In addition, it should be noted that according to the data in Fig. 10, the temperature variation of the AMR in the Ni-Cu/Cu multilayer investigated is very strong, it changes by about a factor 3. This is in agreement with the AMR increase reported for a bulk Ni<sub>81</sub>Cu<sub>19</sub> alloy in the same temperature range.<sup>23</sup>

## Conclusions

We have studied the interrelation between the magnetoresistance and structural quality of ED Ni-Cu/Cu multilayers grown from a sulfate/sulfamate electrolyte for various Ni-Cu and Cu layer thicknesses. MR measurements indicated that the Ni-Cu/Cu multilayers exhibit GMR for most layer thicknesses. Since this is the first report where Ni-Cu/Cu multilayers were prepared with an optimized Cu deposition potential, the true evolution of GMR on layer thicknesses could be traced out.

The variation of GMR with Cu layer thickness was found to be very similar to the case of ED Co-Cu/Cu multilayers<sup>44</sup> in that the GMR increased smoothly with  $d_{Cu}$  up to about 4 nm and decreased afterwards. This indicates clearly the absence of an alternation of AF and FM couplings also for the ED Ni-Cu/Cu multilayers. For sufficiently thick Cu layers, the

magnetic layers are properly separated and become magnetically completely decoupled where a random alignment of adjacent layer magnetizations yields then a GMR effect.

It can be concluded from the present results that there is no firm evidence yet for an oscillatory exchange coupling (and, also, for an oscillatory GMR) as a function of the spacer layer thickness for ED multilayers which is in strong contrast, e.g., with sputtered Co-Ni/Cu multilayers<sup>64</sup> for which a clear oscillatory behavior was reported for the whole concentration range of the magnetic layer. It should be established that there are still some fine structural details of the ED multilayers which are not yet controlled to a sufficient degree. XRD studies on the present multilayers, e.g., have indicated a large fluctuation of the layer thicknesses, particularly in the multilayer series with variable thickness of the spacer layers.

Furthermore, in multilayers with thin Cu layers (below about 1.5 nm), the fluctuations of the spacer layer thickness led to discontinuities in the spacer. These discontinuities can be visualized as pinholes providing a FM bridges between adjacent magnetic layers. As a consequence of the FM coupling via pinholes, the AMR effect characteristic for bulk ferromagnetics dominates the MR behavior in this spacer thickness range.

As to a comparison of the GMR magnitude with results on sputtered multilayers, the GMR is generally smaller in ED multilayers, especially at the first AF maximum. For example, the room-temperature GMR is about 7 % for  $d_{\text{Cu}} \sim 0.9$  nm (first AF maximum) and about 2 % for  $d_{\text{Cu}} \sim 3.2$  nm (third AF maximum) for sputtered Ni/Cu multilayers.<sup>64</sup> With reference to Fig. 1b, one can see that at the expected first AF maximum the ED Ni-Cu/Cu multilayers have a negligible GMR (rather an AMR effect dominates) whereas around the third expected AF maximum position the GMR magnitudes appear as comparable for both the sputtered and the ED multilayers. We should keep in mind, however, that according to the results of Kubota et al.,<sup>64</sup> already 10 at.% Co in the magnetic layer of Ni-Co/Cu multilayers enhances the GMR by about a factor of 2. This practically the case in our multilayers and in most previous studies on ED Ni-Cu/Cu multilayers, no particular attention has been paid to this fact.

It is noted that for very thin Ni-Cu layers, an SPM component to the GMR could be revealed in the ED Ni-Cu/Cu multilayers due to a fragmentation of the magnetic layer. A  $\text{GMR}_{\text{SPM}}$  term could be observed also for high Cu contents in the magnetic layer of multilayers which were deposited from electrolytes with high concentration of  $\text{Cu}^{2+}$  ions. This latter observation indicates that most of the Cu when codeposited in high amount with Ni segregates within the magnetic layer and causes the occurrence of magnetically separated

small FM regions (probably chemically disordered Ni-enriched Ni-Cu alloys) which form SPM entities. This conclusion for phase separation in the Ni-Cu layers of our multilayers is in agreement with theoretically deduced low-temperature phase diagrams and related experimental results on ED Ni-Cu alloys. The chemically heterogeneous nature of the magnetic layer plane, on the other hand, deteriorated the coherent repetition of magnetic and non-magnetic layers and led to the disappearance of multilayer satellites.

As to the temperature dependence of GMR in the ED Ni-Cu/Cu multilayers, a similar GMR increase towards lower temperature was obtained as reported for physically deposited related multilayers.

### **Acknowledgement**

The work of M. Jafari Fesharaki in Hungary was supported by a grant of the Iranian Ministry of Science, Research and Technology. Financial support of the Hungarian Scientific Research Fund (OTKA) through grant # NN 79846 is acknowledged. The closed-cycle He cryostat was kindly donated by the Humboldt Foundation, Germany. The structural studies were performed in frame of the research project RA 1050/11-1 funded by the German Research Foundation (DFG).

## References

1. E.Y. Tsymbal and D.G. Pettifor, *Solid State Phys.* **56**, 113 (2001)
2. M. Angelakeris, E.T. Papaioannou, P. Pouloupoulos, O. Valassiades and N.K. Flevaris, *Sens. Act. A* **106**, 91 (2003)
3. J. Kanak, T. Stobiecki, P. Wisniowski, G. Gladyszewski, W. Maass and B. Szymanski, *J. Magn. Magn. Mater.* **239**, 329 (2002)
4. C.A. Ross, *Ann. Rev. Mater. Sci.* **24**, 159 (1994)
5. W. Schwarzacher and D.S. Lashmore, *IEEE Trans. Magn.* **32**, 3133 (1996)
6. I. Bakonyi and L. Péter, *Progr. Mater. Sci.* **55**, 107 (2010)
7. V. Weihnacht, L. Péter, J. Tóth, J. Pádár, Zs. Kerner, C.M. Schneider and I. Bakonyi, *J. Electrochem. Soc.* **150**, C507 (2003)
8. L. Péter, Q.X. Liu, Zs. Kerner and I. Bakonyi, *Electrochim. Acta* **49**, 1513 (2004)
9. D.S. Lashmore, Y. Zhang, S. Hua, M.P. Dariel, L. Swartzendruber and L. Salamanca-Riba, in: *Magnetic Materials, Processes, and Devices III*. Eds. L.T. Romankiw and D.A. Herman, Jr. (The Electrochemical Society Proceedings Series, Pennington, N.J., 1994), PV 94-6, p. 205.
10. K.D. Bird and M. Schlesinger, *J. Electrochem. Soc.* **142**, L65 (1995)
11. I. Bakonyi, E. Tóth-Kádár, T. Becsei, J. Tóth, T. Tarnóczy, Á. Cziráki, I. Gerócs, G. Nabyouni and W. Schwarzacher, *J. Magn. Magn. Mater.* **156**, 347 (1996)
12. Á. Cziráki, I. Gerócs, B. Fogarassy, B. Arnold, M. Reibold, K. Wetzig, E. Tóth-Kádár and I. Bakonyi, *Z. Metallkde.* **88**, 781 (1997)
13. K.C. Liddell and Z. Liu, in: *Proc. Symposium on Aqueous Electrotechnologies - Progress in Theory and Practice* (TMS, Warrendale, Pa. U.S.A., 1997), p. 443
14. M. Shima, L. Salamanca-Riba and L.J. Swartzendruber, *Mater. Res. Soc. Symp. Proc.* **451**, 419 (1997)
15. J. Tóth, L.F. Kiss, E. Tóth-Kádár, A. Dinia, V. Pierron-Bohnes and I. Bakonyi, *J. Magn. Magn. Mater.* **198-199**, 243 (1999)
16. N.V. Myung and K. Nobe, *Plat. Surf. Fin.* **87(6)**, 125 (June 2000)
17. N.V. Myung, M. Schwartz and K. Nobe, in: *Fundamental Aspects of Electrochemical Deposition and Dissolution*. Eds. M. Matlosz, D. Landolt, R. Aogaki, Y. Sato and J.B. Talbot (The Electrochemical Society Proceedings Series, Pennington, NJ, USA, 2000), PV 99-33, p. 263.
18. E. Tóth-Kádár, L. Péter, T. Becsei, J. Tóth, L. Pogány, T. Tarnóczy, P. Kamasa, I. Bakonyi, G. Láng, Á. Cziráki and W. Schwarzacher *J. Electrochem. Soc.* **147**, 3311 (2000)
19. I. Bakonyi, J. Tóth, L. Goualou, T. Becsei, E. Tóth-Kádár, W. Schwarzacher and G. Nabyouni. *J. Electrochem. Soc.* **149**, C195 (2002)
20. A. Tokarz, A. Wolkenberg and T. Przeslawski, *J. Electrochem. Soc.* **149**, C607 (2002)
21. A. Tokarz, Z. Nitkiewicz and A. Wolkenberg, *Electron Technology – Internet Journal* **35(5)**, 1 (2003)
22. M. Alper, M.C. Baykulb, L. Péter, J. Tóth and I. Bakonyi, *J. Appl. Electrochem.* **34**, 841 (2004)
23. I. Bakonyi, J. Tóth, L.F. Kiss, E. Tóth-Kádár, L. Péter and A. Dinia, *J. Magn. Magn. Mater.* **269**, 156 (2004)
24. I. Kazeminezhad and W. Schwarzacher, *J. Solid State Electrochem.* **8**, 187 (2004)
25. W.R.A. Meuleman, S. Roy, L. Péter and I. Bakonyi, *J. Electrochem. Soc.* **151**, C256 (2004)
26. A. Mallik and B.C. Ray, in: *Proc. 4th Asian Advanced Particle Technology* (New Delhi, 2009). National Institute of Technology - Rourkela, India, available at: <http://hdl.handle.net/2080/1059>
27. G.R. Nabyouni, *Metrol. Meas. Syst.* **16**, 519 (2009)
28. F.L. Zhu, Q.Q. Yu, D. Huang and J.P. Xie, *New Technology & New Process (China)*, No. 1, 88 (2009)

29. Y.W. Rheem, *Kor. J. Mater. Res.* **20**(2), 90 (2010)
30. S.K. Ghosh, S. Singh and S. Basu, *Mater. Chem. Phys.* **120**, 199 (2010)
31. S.M.S.I. Dulal and E.A. Charles, *J. Phys. Chem. Sol.* **71**, 309 (2010)
32. L. Péter and I. Bakonyi, Chapter 12 in: *Electrocrystallization in Nanotechnology*. Ed. G. Staikov (Wiley-VCH, Weinheim, Germany, 2007), p. 242.
33. L. Péter, J. Pádár, E. Tóth-Kádár, Á. Cziráki, P. Sóki, L. Pogány and I. Bakonyi, *Electrochim. Acta* **52**, 3813 (2007)
34. D. Rafaja, C. Schimpf, V. Klemm, G. Schreiber, I. Bakonyi and L. Péter, *Acta Mater.* **57**, 3211 (2009)
35. D. Rafaja, C. Schimpf, T. Schucknecht, V. Klemm, L. Péter and I. Bakonyi, *Acta Mater.* **59**, 2992 (2011)
36. D. Rafaja, H. Fuess, D. Šimek, L. Zdeborová and V. Valvoda, *J. Phys.: Condens. Matter* **14**, 10021 (2002)
37. E.E. Fullerton, I.K. Schuller, H. Vanderstraeten and Y. Bruynserade, *Phys. Rev. B* **45**, 9292 (1992)
38. K.E. Meyer, G.P. Felcher, S.K. Sinha and I.K. Schuller, *J. Appl. Phys.* **52**, 6608 (1981)
39. C. Michaelsen, *Philos. Mag. A* **72**, 813 (1995)
40. R.M. Bozorth, *Ferromagnetism* (Van Nostrand, New York, 1951)
41. T.R. McGuire and R.I. Potter, *IEEE Trans. Magn.* **11**, 1018 (1975)
42. B.G. Tóth, L. Péter, Á. Révész, J. Pádár and I. Bakonyi, *Eur. Phys. J. B* **75**, 167 (2010)
43. J.F. Bobo, H. Kikuchi, O. Redon, E. Snoeck, M. Piecuch and R. L. White, *Phys. Rev. B* **60**, 4131 (1999)
44. I. Bakonyi, E. Simon, B.G. Tóth, L. Péter and L.F. Kiss, *Phys. Rev. B* **79**, 174421 (2009)
45. A. Vernes, H. Ebert and J. Banhart, *Phys. Rev. B* **68**, 134404 (2003)
46. I. Bakonyi, E. Tóth-Kádár, J. Tóth, T. Becsei, L. Pogány, T. Tarnóczi and P. Kamasa, *J. Phys.: Cond. Matter* **11**, 963 (1999)
47. I. Bakonyi, L. Péter, Z. Rolik, K. Kiss-Szabó, Z. Kupay, J. Tóth, L. F. Kiss and J. Pádár, *Phys. Rev. B* **70**, 054427 (2004)
48. M. Shima, L.G. Salamanca-Riba, R.D. McMichael and T.P. Moffat, *J. Electrochem. Soc.* **148**, C518 (2001)
49. C.H. Marrows and B.J. Hickey, *Phys. Rev. B* **59**, 463 (1999)
50. Q.X. Liu, L. Péter, J. Pádár and I. Bakonyi, *J. Electrochem. Soc.* **152**, C316 (2005)
51. T.B. Massalski (Ed.), *Binary Alloy Phase Diagrams*, Second Edition Plus Updates on CD-ROM (ASM International, Materials Park, Ohio, USA, 1996)
52. D.J. Chakrabarti, D.E. Laughlin, S.W. Chen and Y.A. Chang, in: *Phase Diagrams of Binary Nickel Alloys*. Ed. P. Nash (ASM International, Materials Park, OH, 1991)
53. C.P. Wang, X.J. Liu, M. Jiang, I. Ohnuma, R. Kainuma and K. Ishida, *J. Phys. Chem. Sol.* **66**, 256 (2005)
54. T.J. Hicks, B. Rainford and J.S. Kouvel, *Phys. Rev. Lett.* **22**, 531 (1969)
55. J.S. Kouvel and J.B. Comly, *Phys. Rev. Lett.* **24**, 598 (1970)
56. A. Amamou, F. Gautier and B. Loegel, *J. Phys. F* **5**, 1342 (1975)
57. T. Tsakalacos, *Scripta Metallurg.* **15**, 255 (1981)
58. I. Kazeminezhad and W. Schwarzacher, *J. Magn. Magn. Mater.* **226-230**, 1650 (2001)
59. S.K. Ghosh, A.K. Grover, G.K. Dey, U.D. Kulkarni, R.O. Dusane, A.K. Suri and S. Banerjee, *J. Mater. Res.* **21**, 45 (2006)
60. Zhu Liu, Lian Guo, Chia-Ling Chien, and P.C. Searson, *J. Electrochem. Soc.* **155**, D569 (2008)
61. I. Mizushima, M. Chikazawa and T. Watanabe, *J. Electrochem. Soc.* **143**, 1978 (1996)
62. H. Kubota, M. Sato and T. Miyazaki, *Phys. Rev. B* **52**, 343 (1995)
63. H. Hasegawa, *Phys. Rev. B* **47**, 15080 (1993)
64. H. Kubota, S. Ishio, T. Miyazaki and Z.M. Stadnik, *J. Magn. Magn. Mater.* **129**, 383 (1994)

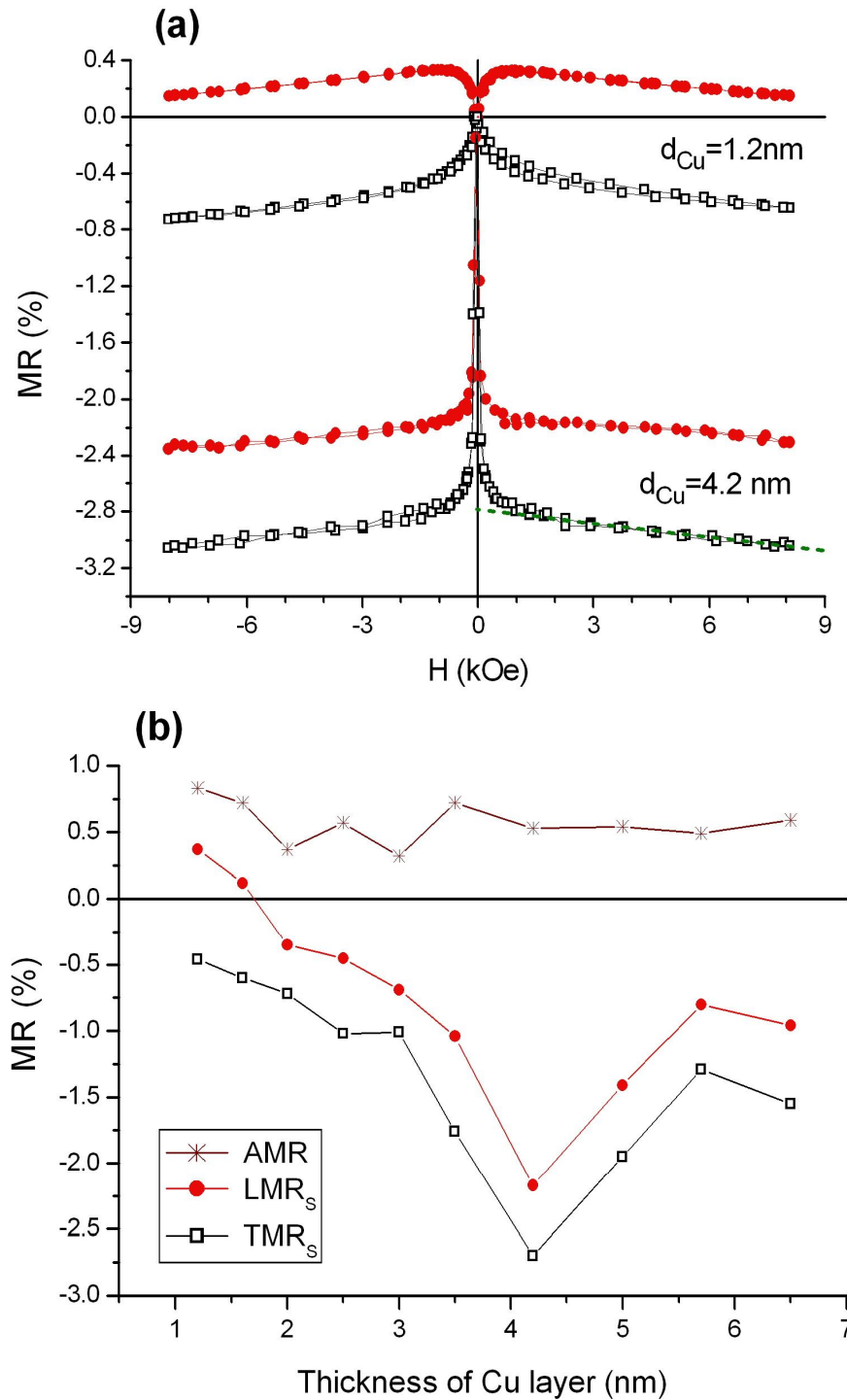


Fig. 1 (a) LMR (closed symbols) and TMR (open symbols) magnetoresistance curves of ED Ni-Cu/Cu multilayers from series B which were prepared with  $d_{Ni-Cu} = 3 \text{ nm}$  and with Cu layer thicknesses as indicated. The extrapolation of the MR(H) curves to  $H = 0$  as indicated by the dashed line for one of the TMR components served for the determination of the saturation magnetoresistance values ( $LMR_s$  and  $TMR_s$ ); (b) Evolution of the  $LMR_s$  and  $TMR_s$  components and the AMR magnitude with Cu layer thickness for ED Ni-Cu/Cu multilayers (series B) with constant magnetic layer thickness ( $d_{Ni-Cu} = 3 \text{ nm}$ ).

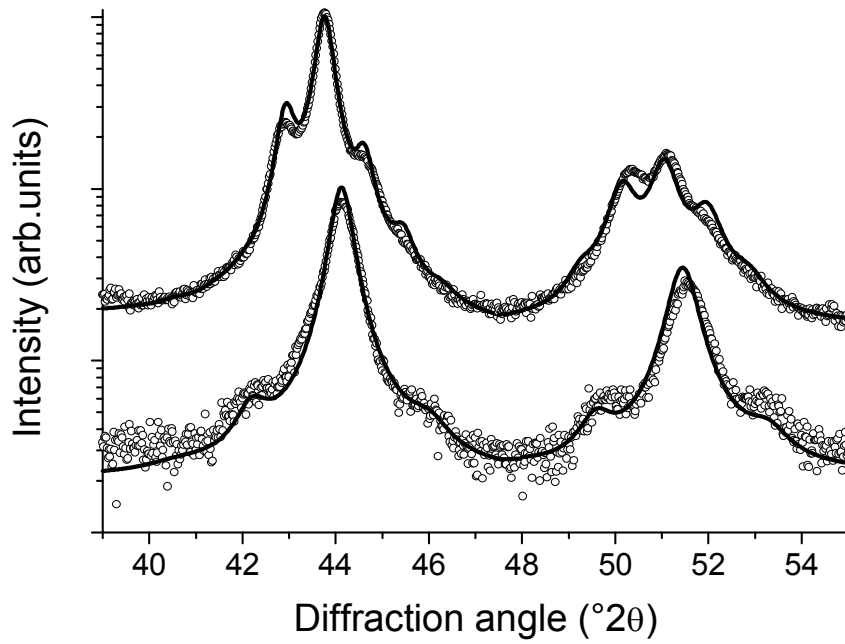


Fig. 2 XRD patterns of the Ni-Cu(3nm)/Cu(1.2nm) (lower curves) and Ni-Cu(3nm)/Cu(6.5nm) (upper curves) multilayers. The measured data are plotted by open circles, the intensities simulated in the vicinity of the diffraction lines 111 (left) and 200 (right) by solid lines. All intensities are plotted in logarithmic scale. For simulation, the routine from Ref. 36 was applied.

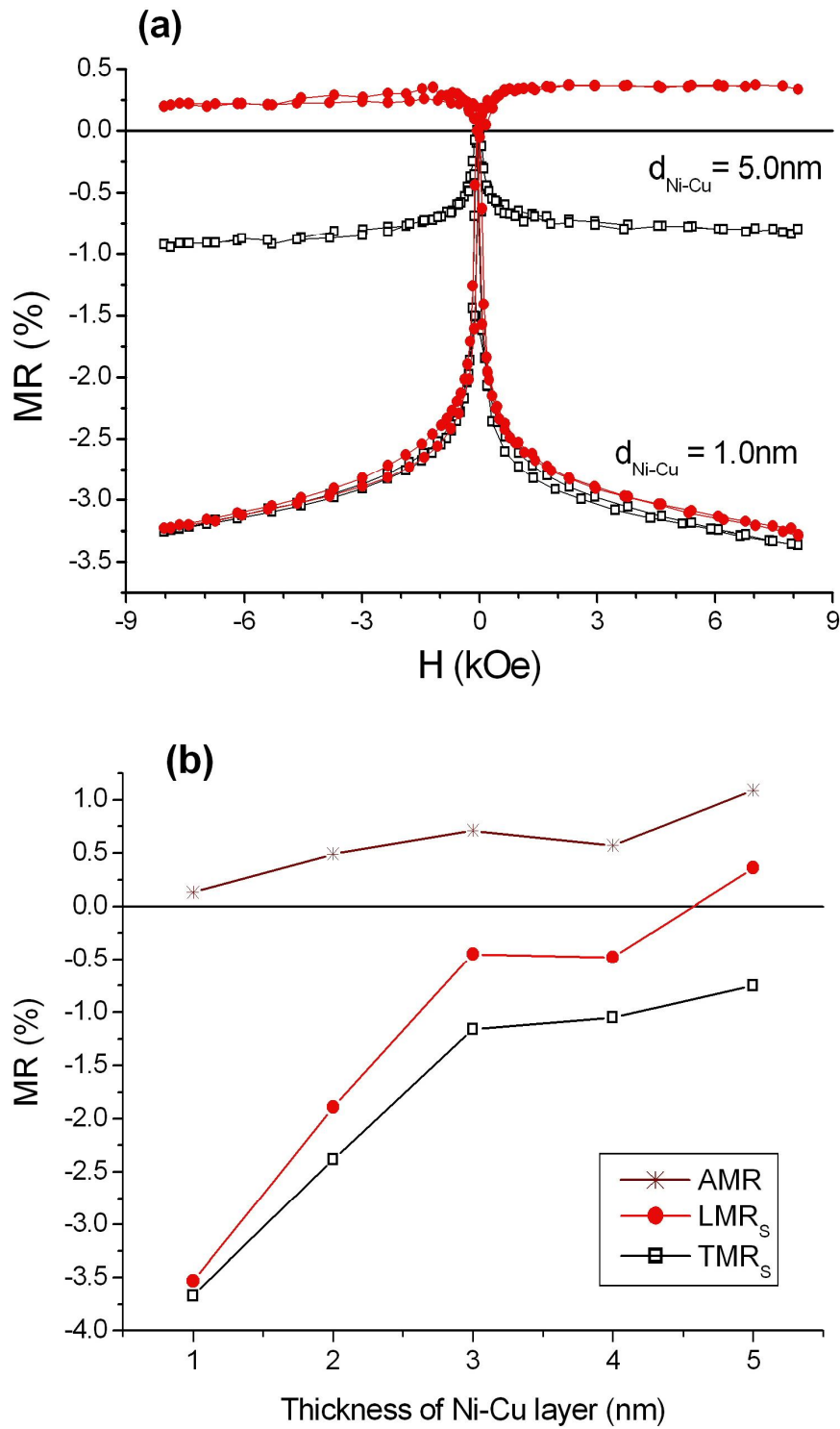


Fig. 3 (a) LMR (closed symbols) and TMR (open symbols) magnetoresistance curves of ED Ni-Cu/Cu multilayers from series H which were prepared with constant Cu layer thickness ( $d_{\text{Cu}} = 4.2 \text{ nm}$ ) and with magnetic layer thicknesses as indicated in the figure. (b) Evolution of the LMR<sub>S</sub> and TMR<sub>S</sub> values and the AMR magnitude with Ni-Cu layer thickness for the ED Ni-Cu/Cu multilayer series H with constant non-magnetic layer thickness ( $d_{\text{Cu}} = 4.2 \text{ nm}$ ). For the multilayer with  $d_{\text{Ni-Cu}} = 1 \text{ nm}$ , the LMR<sub>S</sub> and TMR<sub>S</sub> values were obtained as described in the text.

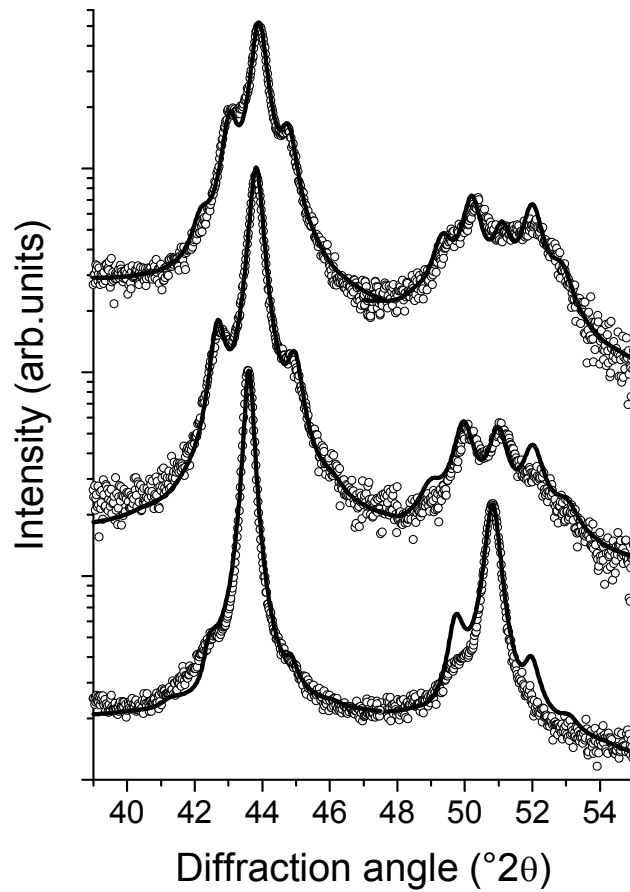


Fig. 4 XRD patterns of the Ni-Cu(5nm)/Cu(4.2nm) (top), Ni-Cu(3nm)/Cu(4.2nm) (middle) and Ni-Cu(1nm)/Cu(4.2nm) (bottom) multilayers. The measured data are plotted by open circles, the intensities simulated in the vicinity of the diffraction lines 111 (left) and 200 (right) by solid lines. All intensities are plotted in logarithmic scale.

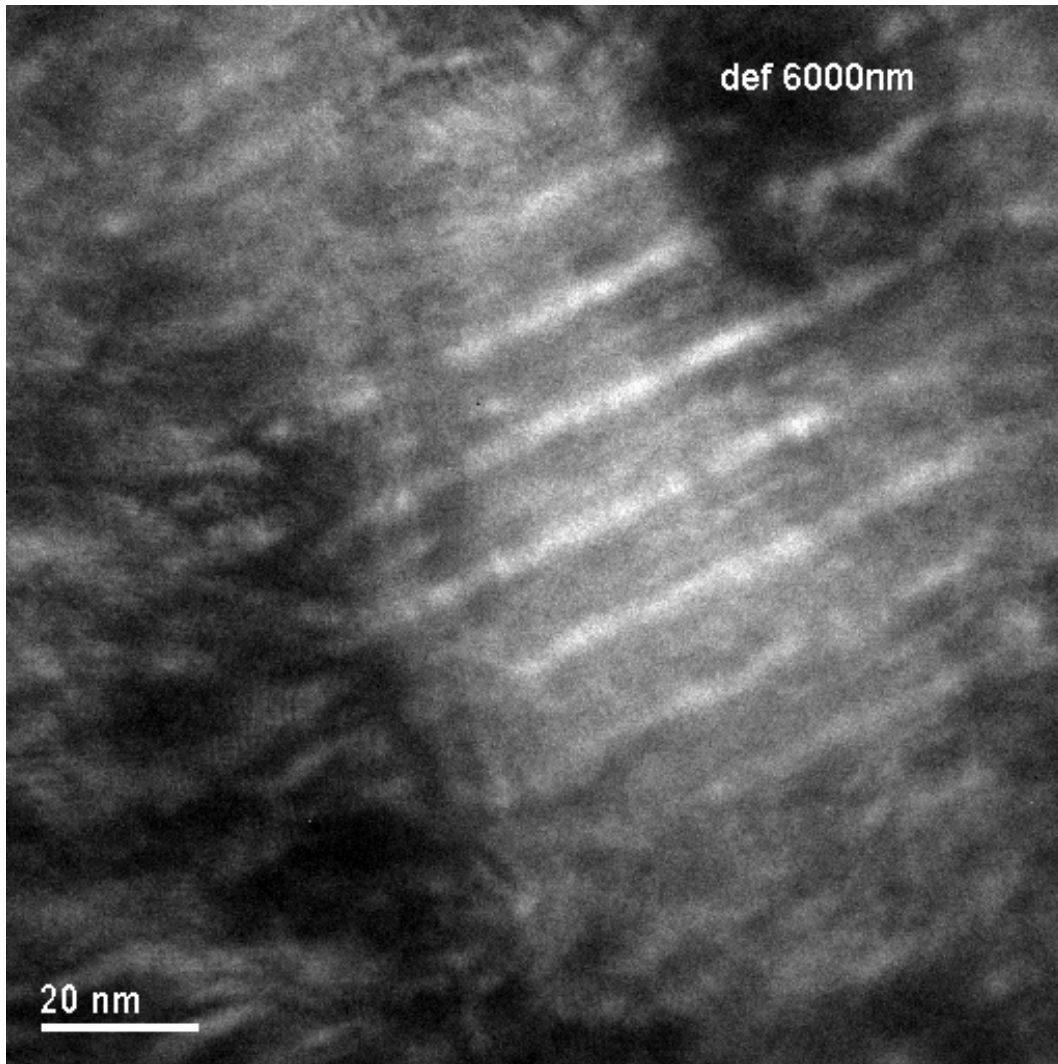


Fig. 5 Cross-sectional TEM image of the ED Ni-Cu(3.0nm)/Cu(4.2nm) multilayer from series H. Due to the strong defocus necessary to create sufficient contrast between the Ni and Cu layers, the scale-bar is only approximate.

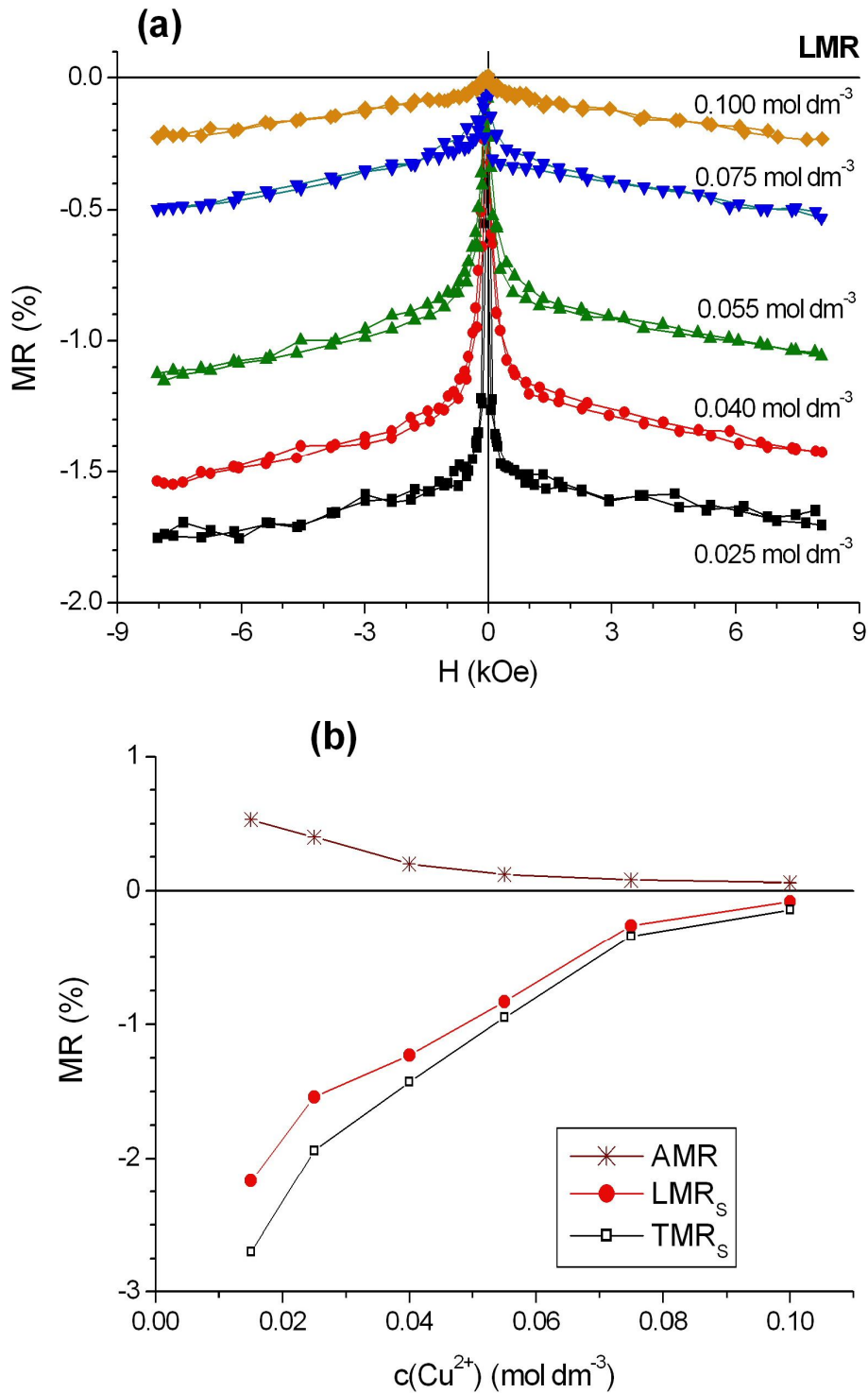


Fig. 6 (a) Evolution of the LMR(H) curves for some selected multilayers in series G with  $d_{\text{Ni-Cu}} = 3$  nm and  $d_{\text{Cu}} = 4.2$  nm (the figures attached to the curves indicate the  $\text{Cu}^{2+}$  concentration in the bath). The TMR(H) curves were very similar just with somewhat higher MR values; (b) Evolution of the LMR<sub>s</sub> (closed symbols) and TMR<sub>s</sub> (open symbols) values and the AMR magnitude with  $\text{Cu}^{2+}$  ion concentration in the bath for these ED Ni-Cu/Cu multilayer series G.

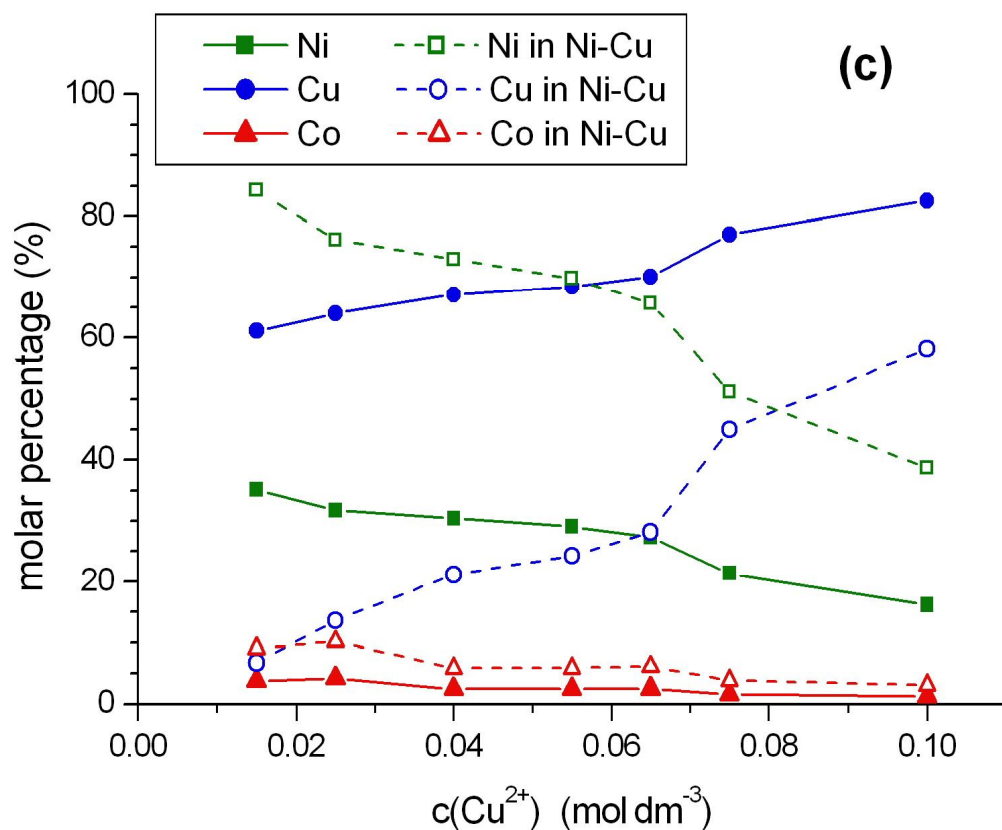


Fig. 7 Results of chemical composition analysis of multilayer series G as a function of the  $\text{Cu}^{2+}$  ion concentration in the bath. The full symbols indicate analyzed overall compositions whereas open symbols give composition data calculated for the magnetic layers only.

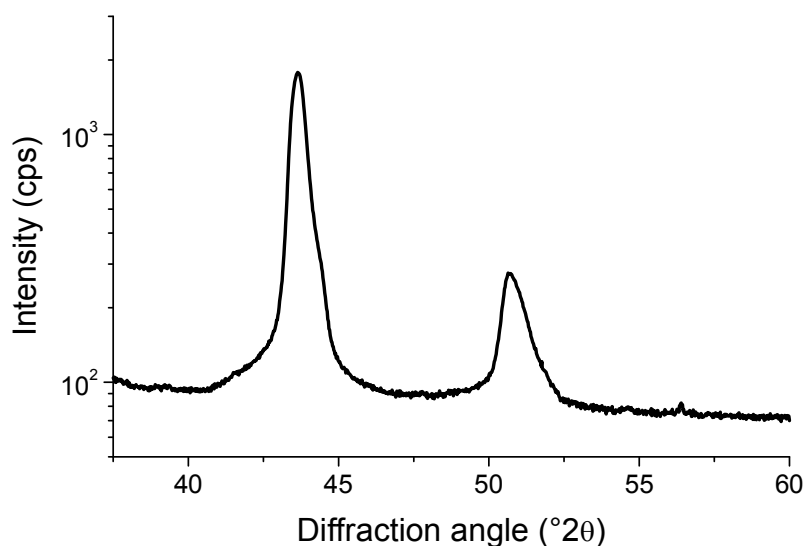


Fig. 8 XRD pattern of the ED Ni-Cu(3.0nm)/Cu(4.2nm) multilayer from series G which was prepared from a bath containing the highest concentration ( $0.1 \text{ mol/dm}^3$ ) of  $\text{Cu}^{2+}$  ions. The XRD result is consistent with a material in which Cu is the dominant phase and Ni as the minor phase.

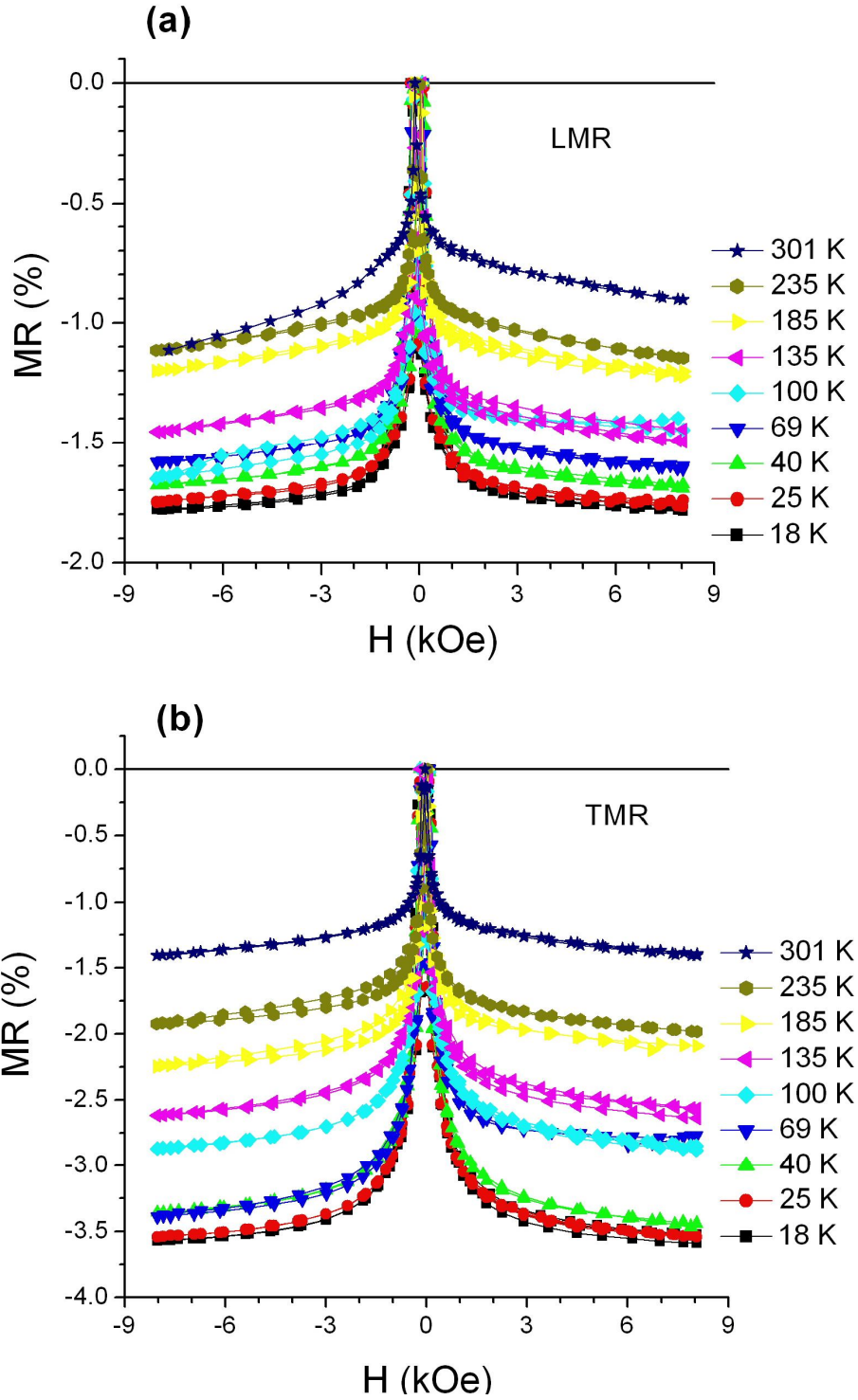


Fig. 9 Temperature dependence of the (a) LMR(H) and (b) TMR(H) curves for an ED Ni-Cu(3nm)/Cu(5nm) multilayer from series B.

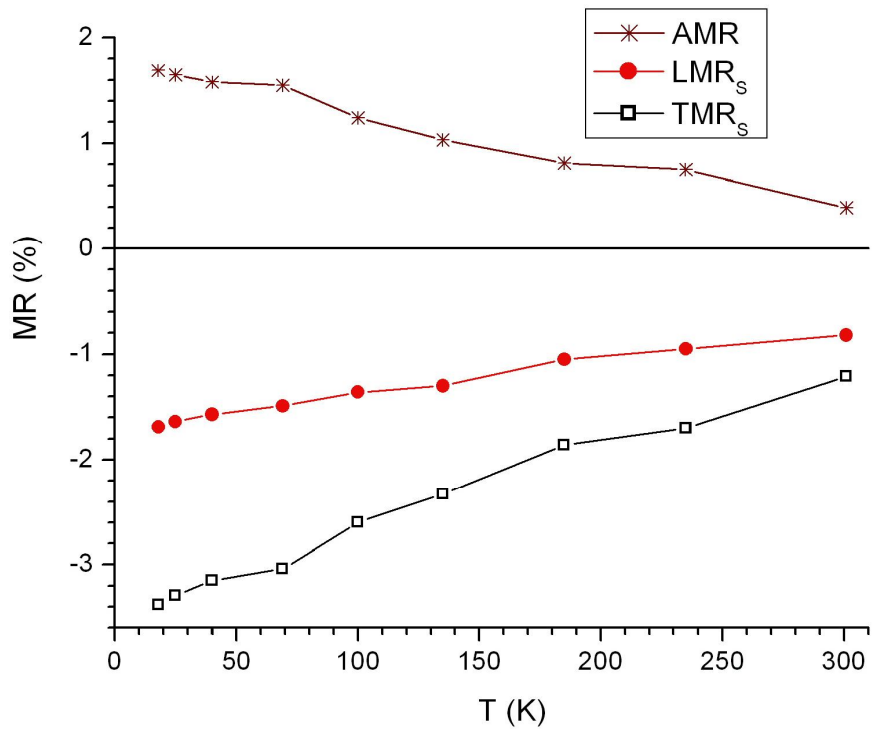


Fig. 10 Temperature dependence of the LMR<sub>S</sub> and TMR<sub>S</sub> values and the AMR magnitude for the ED Ni-Cu/Cu multilayer of Fig. 9.